UNIVERSITY OF TARTU
Faculty of Science and Technology
Institute of Technology

Aleksandr Illarionov

Quantitative evaluation of sodium and potassium salts stress in yeasts

Bachelor's Thesis (12 ECTS)

Curriculum Science and Technology

Supervisor(s):
Researcher, PhD Rahul Kumar
Senior researcher, PhD Petri-Jaan Lahtvee

Tartu 2020

Quantitative evaluation of sodium and potassium salts stress in yeasts

Abstract:

Saline stress is commonly encountered by microbial cell factories. The molecular mechanisms of saline stress are identified in the conventional budding yeast *Saccharomyces cerevisiae* that is used in biotechnology. However, for diversification of microbial cell factories, non-conventional yeasts provide an attractive opportunity but saline stress in these yeasts is not very well investigated. This thesis is focused on achieving foundational understanding of morphological and physiological response to saline stress of conventional and non-conventional yeasts by comparing *Saccharomyces cerevisiae* W303 and CEN.PK113-7D together with *Kluyveromyces marxianus* and *Rhodotorula toruloides*. The results showed that effects of Na^+ stress could be ameliorated by potassium supplementation in *S. cerevisiae* CEN.PK113-7D increasing its specific growth rate by almost four-fold. In addition, combination of sodium and potassium salts resulted in impaired acetic acid and/or ethanol metabolism in *S. cerevisiae*. Further, in this thesis, a neural network-based image analysis software pipeline for a quantitative evaluation of saline stress response was developed that could be used to determine differences in cell volume among the strains. Quantitative image analysis found a high variability in cell volume dynamics implying distinct stress response mechanisms among different yeasts. The cell volume differences could be used to model saline stress responses in various bioprocesses in biotechnology.

Keywords:

Saccharomyces cerevisiae; *Kluyveromyces marxianus*; *Rhodosporidium toruloides*; yeast; non-conventional yeast; salt stress; osmotic stress; biotechnology; image analysis

CERCS:

T490 Biotechnology

Naatrium- ja kaaliumsoolade stressi kvantitatiivne analüüs pärmides

Lühikokkuvõte:

Kõrgete soola kontsenteratsioonide poolt põhjustatud osmootne stress on levinud stressifaktor tööstuslikult kasutavatele mikroorganismidel põhinevatele rakuvabrikutele. Soola stressi molekulaarsed mehhanismid on tuvastatud tavapärases punguvas pärmis *Saccharomyces cerevisiae*, mida kasutatakse biotehnoloogias. Mittekonventsionaalsed pärmid kujundavad endast atraktiivset võimalust mikrobioloogiliste rakuvabrikute diversifitseerimiseks, kuid soola stress sellistes pärmides on tänini praktiliselt kirjeldamata. Käesoleva bakalaureusetöö eesmärk on fundamentaalse arusaama saavutamine konventsionaalsete ja mittekonventsionaalsete pärmide ja nende soola stressi morfoloogilise ja füsioloogilise vastuste suhtes. Võrdluseks on kasutatud *Saccharomyces cerevisiae* CEN.PK113-7D ja W303, *Kluyveromyces marxianus* ja *Rhodotorula toruloides* pärmide tüvesid. Tulemused näidavad, et naatriumi tingitud stressi effektid võib leevendada kaaliumi lisamisega pärmis *S. cerevisiae* CEN.PK113-7D, peaaegu neljakordistades tema erikasvukiirust. Lisaks, naatriumi ja naatriumi/kaaliumi kombinatsioonid põhjustasid nõrgenenud atsetaadi ja/või etanooli metabolismi pärmis *S. cerevisiae*. Peale selle, tehisnärvivõrgul põhinev pilditöötluse tarkvara oli välja töötatud soola stressist põhjustatud rakkude ruumala muutuste kvantitatiivseks analüüsiks. Kvantitatiivne piltide analüüs on leidnud suurt variatiivsust rakkude mahus, vihjates eristuvatele stressile vastuste mehhanismidele erinevates pärmides. Rakkude mahu erinevusi võib kasutada soola stressile vastuste modelleerimiseks mitmesugustes biotehnoloogia bioprotsessides.

Võtmesõnad:

Saccharomyces cerevisiae; *Kluyveromyces marxianus*; *Rhodotorula toruloides*; pärm; mittekonventsionaalne pärm; soola stress; osmootiline stress; biotehnoloogia; pilditöötlus

CERCS:

T490 Biotehnoloogia

TABLE OF CONTENTS

ABBREVIATIONS

SCW – Saccharomyces cerevisiae W303

SCP – Saccharomyces cerevisiae CEN.PK113-7D

KM – Kluyveromyces marxianus

RT– Rhodotorula toruloides

INTRODUCTION

Microbial cell factories are considered important for an environmentally sustainable future. Microbial factories are based on genetically engineered microorganisms, which could meet chemical production demands using bioprocesses instead of fossil-fuel dependent chemical synthesis processes. (Nielsen, 2015) These microorganisms should have a high tolerance towards industrial stresses like temperature, pH, osmotic stress. (Hohmann, 2002b; Lahtvee *et al.*, 2016) In this thesis, two key mineral nutrients i.e., sodium (Na^+) and potassium (K^+), which are present as monovalent cations in the culture environment of yeasts were selected for investigation. These cations can be harmful in high concentrations due to osmotic stress and direct toxicity. (Lam *et al.*, 2014; Lahtvee *et al.*, 2016)

Homeostasis of Na^+ and K^+ is vital for survival of yeasts and concerns to better understand the response to salt stress has led to an extensive research focus using pulse change experiments. (Rodríguez-Navarro, 2000; Hohmann, 2002; Arino *et al.*, 2010) However, the physiological responses to adaptive salt stress of yeasts together with an interplay of Na^+ and K^+ have not been well investigated.

This thesis addresses adaptive salt stress and the interplay of Na^+ and K^+ using two *Saccharomyces cerevisiae* strains, i.e. W303 and CEN.PK113-7D, as well as two industrially relevant non-conventional yeasts: *Kluyveromyces marxianus* and *Rhodotorula toruloides*. *K. marxianus* has close evolutionary origin to *S. cerevisiae*, while *R. toruloides* has a distant evolutionary origin (Figure 1). Design of this study allowed to look at the generic salt stress responses in yeasts.

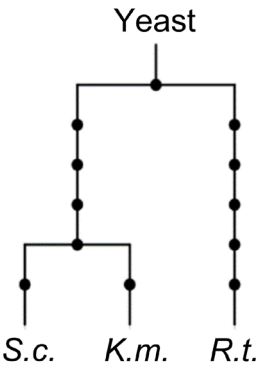

Figure 1. Phylogenetic tree

Briefly, results showed that cell volume response to salt stress not only depended on an applied stressor, but also on the genetic background of yeasts. Further results showed that sensitivity of CEN.PK to sodium can be ameliorated to a degree by addition of K^+ to a culture medium. To gain a quantitative understanding of saline stress response, a neural network-based image analysis software pipeline was developed and applied in this thesis, which allowed for comparison of cell volume distributions among different yeasts.

1 LITERATURE REVIEW

1.1 Yeasts – origins and applications

S. cerevisiae is frequently found in fruits, insects and humans as a commensal. (Goddard and Greig, 2015) Being a unicellular eukaryote, it serves as a model organism to understand mechanisms of human diseases and is conventionally used as a microbial cell factory. *S. cerevisiae* W303 strain is generally used in biomedical research and is partially derived from another popular yeast strain S288C. (Ralser *et al.*, 2012) CEN.PK line of strains emerged as an alternative to S288C and is often used for metabolic modelling as well as a cell factory. (Strucko *et al.*, 2015) Metabolites such as ethanol, as well as proteins like insulin, are commercially produced using *S. cerevisiae*. (Ostergaard et al, 2000)

K. marxianus strains were isolated from a great variety of environments providing a high metabolic diversity and making it a promising candidate for the applications in the future cell factories. The strain used in this study was isolated from Mexican fermented corn dough. (Fonseca *et al.*, 2008; Jeong *et al.*, 2012) *K. marxianus* is mostly used for ethanol production from food waste streams. (Satyanarayana and Kunze, 2017)

R. toruloides is an oleaginous yeast that is found in a wide variety of habitats, including surfaces of leaves, soil, and seawater. A broad substrate range and ability to accumulate lipids and carotenoids makes it a promising cell factory. (Park *et al.*, 2018; Tiukova *et al.*, 2019) The strain used in this thesis was actively investigated for production of carotenoids. (Azambuja *et al.*, 2018)

Yeasts can be characterized into Crabtree positive, like *S. cerevisiae* and Crabtree negative, like *K. marxianus* and *R. toruloides*. (Bruinenberg *et al.*, 1986, Wardrop *et al.*, 2004) Crabtree effect, also known as overflow metabolism, is characterized by incomplete oxidation of carbon sources and formation of by-products like ethanol, acetic acid and glycerol. Formation of by-products is essential for recycling of excessive NADH that cannot be turned into energy by respiration. (Kumar and Lahtvee, 2020)

1.2 Osmoregulation in yeasts

Osmoregulation consists of active processes that a cell uses to monitor and adjust osmotic pressure, turgor, relative water content and shape. The budding yeast *S. cerevisiae* is a key model organism used to understand osmoregulation. (Klipp *et al.*, 2005) However, due to evolutionary conservation of proteins and pathways involved in osmotic regulation similar

mechanisms can be found in other yeasts. (Qian *et al.*, 2011; Bommareddy *et al.*, 2017) Yeasts contain four systems involved in osmoregulation: aquaglyceroporins, protein kinase C pathway (PKC), and the high osmolarity glycerol (HOG) pathway. (Hohmann, 2002a) Additionally, *K. marxianus* and *R. toruloides* have a functional system of aquaporins that is non-functional in *S. cerevisiae*. (Ahmadpour *et al.*, 2014)

Aquaglyceroporins are glycerol channels which are also permeable to acetic acid. Their main role is to mediate glycerol efflux during active growth. The ability to mediate glycerol efflux is also essential for survival during hypoosmotic stress by keeping the difference between internal and external osmolarity within an optimal range by changing internal glycerol concentration. (Ahmadpour *et al.*, 2014)

Protein kinase C (PKC) pathway regulates cell wall integrity. It is essential for hypoosmotic stress tolerance. The pathway reinforces the cell wall upon decrease in a growth medium osmolarity by activating genes involved in cell wall biosynthesis. (Hohmann, 2002a)

Aquaporins are water channels that play a role in maintaining cellular water homeostasis. Aquaporins mediate freeze tolerance, but as a trade-off also increases sensitivity to osmotic cycles, which are frequently encountered in laboratory settings. As a result, some or all aquaporins are frequently non-functional in laboratory strains. (Ahmadpour *et al.*, 2014)

The high osmolarity glycerol (HOG) pathway is a mitogen-activated protein (MAP) kinase pathway that is essential for hyperosmotic stress tolerance. It activates production of glycerol as well as its retention. (Hohmann, 2002a) Since HOG pathway is the main regulator of hyperosmotic stress tolerance, it is of high relevance for this thesis.

1.2.1 Osmotic stress, cell volume and HOG pathway kinetics

Sorbitol, as well as salts of potassium and sodium are frequently used as stressors to study the effects of osmotic stress. Sorbitol is a non-metabolizable non-permeable sugar alcohol with mostly osmotic effects. (Nass and Rao, 1999, Mitchell, Wei and Lim, 2015) Potassium has low toxicity and, therefore, causes mostly osmotic stress as well. (Serrano, 1996) Sodium has a much higher toxicity than potassium due to its ability to substitute potassium and magnesium in enzymes, like Met22p and Inm1/2p, which are involved in methionine and inositol biosynthesis. (Lopez *et al.*, 1999, Albert *et al.*, 2000)

Cell volume is an important biophysical property and, therefore, many studies have monitored cell volume dynamics during osmotic stress. (Schaber *et al.*, 2010) Microfluidic devices are commonly used to follow cell volume after a change in growth medium

osmolarity. They also allow to monitor the activity of the HOG pathway by monitoring localisation of a Hog1p linked fluorescent protein, which is cytoplasmic under normal conditions and nuclear under osmotic stress. (Petelenz-Kurdziel *et al.*, 2011) The studies reviewed were mostly performed in *S. cerevisiae* S288C, W303 or their derivatives which are considered as the model strains for studying osmotic stress. Due to frequent prevalence of hyperosmotic environments the HOG pathway regulation was extensively studied by use of pulse response monitoring in yeasts for up to one hour which was sufficient for the activation and adaptation of HOG pathway. (Mitchell, Wei and Lim, 2015) Studies that focused on adapted strains were mostly concerned with their growth rates at different conditions. (Petelenz-Kurdziel *et al.*, 2011; Babazadeh *et al.*, 2013, 2017)

These studies showed that osmotic changes are monitored through a plasma membrane protein Sln1p, which actively represses the HOG pathway in *S. cerevisiae*. Sln1p is inactivated upon loss of turgor pressure and results in the activation of MAP kinase cascade and phosphorylation of Hog1p. (Klipp *et al.*, 2005) A decrease in volume prompts activation of the HOG pathway, which culminates in phosphorylation of Hog1p that subsequently accumulates in the nucleus. Hog1p controls the activity of the glycerol channel Fps1p as well as gene expressions through activation of transcription factors Msn2p and Hot1p. Msn2p is a general stress response transcription factor required for transcription of many stress-induced genes. (Hohmann, 2002b)

Hot1p induces expression of *GPD1* and *GPD2* genes, which encode enzymes involved in the production of glycerol. (Hohmann, 2002b) However, glycerol production is carbon source dependent, and trehalose is produced instead when cells are grown on a respiratory carbon source like ethanol instead of a fermentative one like glucose. HOG pathway induction is much weaker on a respiratory carbon source and, therefore, cell volume recovers slower. (Babazadeh *et al.*, 2017)

Activation of the HOG-pathway is transient. This allows cells to remain responsive to potential changes in osmolarity of growth medium. The full course of activation and adaptation of the Hog1p takes about 30 minutes with an activation peak at around 5 minutes in the pulse experiments. (Babazadeh *et al.*, 2013; Mitchell *et al.*, 2015)

Volume reduction caused by osmotic stress is mostly due to water efflux. All cell compartments do not recover volume at the same pace, for example, nuclear volume recovery happens much faster than recovery of cytosol. (Petelenz-Kurdziel *et al.*, 2011) Cell volume decrease causes decrease in diffusion speed. This increases the concentration of

molecules inside a cell resulting in molecular overcrowding, which reduces the rate of cellular processes. The extent of cell volume decrease influences the speed of adaptive response due to reduced rate of cellular processes. (Babazadeh *et al.*, 2013) Due to this, osmotic stress causes a delay in the G1 phase, which is when a cell accumulates resources and energy to start cell division. (Bellí *et al.*, 2001) Cell volume in reviewed studies was able to return to normal only when cells were exposed to up to a certain increase in osmolarity of the growth medium. Cells were not able to regain initial volume in case of NaCl concentrations of more than 0.6 M, at least during the studied timeframe of 45 minutes. (Petelenz-Kurdziel *et al.*, 2011; Babazadeh *et al.*, 2013)

1.3 Cationic homeostasis and salt tolerance

Growth media contain different dissolved salts and other nutrients. Yeasts have evolved mechanisms to regulate salt homeostasis. Sodium and potassium are two of the most abundant salt cations in common growth media. Potassium is an essential micronutrient required for maintenance of membrane potential, intracellular pH, cell volume and enzyme activity. (Herrera *et al.*, 2014, Yenush, 2016b) Concentrations of around 0.5 mM are required for optimal growth of *S. cerevisiae*. (Camacho and Ramos, 1981) Yeasts, as many other organisms, maintain a high potassium/sodium ratio by selective potassium uptake and extrusion or vacuole sequestration of sodium ions. The resulting gradient of sodium ions is then used by secondary transporters for coupled uptake of other ions and nutrients. A proton motive force is required for most of these transport processes and the plasma membrane transporter, Pma1p, is responsible for maintaining the proton gradient. Intracellular pH and presence of glucose regulate the Pma1p activity. (Yenush, 2016b)

Yeasts can tolerate high external salt concentrations due to the presence of plasma membrane located $H^+/Na^+(K^+)$ antiporter Nha1p, ATP-dependent $Na^+(K^+, Li^+)$ pumps Ena(1-6)p and a voltage-gated K^+ channel Tok1p, all of which can remove cations out of a cell for maintaining homeostasis. Yeast also have a vacuolar $H^+/Na^+(K^+)$ antiporter Nhx1p, which is important for acute salt stress tolerance as it sequesters sodium and potassium ions in a vacuole. These pumps and channels allow yeasts to keep optimal internal potassium concentration as well as high potassium/sodium ratio. (Yenush, 2016a)

2 THE AIMS OF THE THESIS

The aims of this thesis are to:

1. Investigate physiological response of conventional yeasts to adaptive salt stress (NaCl, KCl – both individually and together)
2. Develop a quantitative evaluation tool for monitoring morphological changes using microscopic images
3. Provide a foundational comparison of adaptive salt stress response in conventional and non-conventional yeasts

3 EXPERIMENTAL PART

3.1 MATERIALS AND METHODS

3.1.1 Strains and culture conditions

The following strains were used in this thesis: *Saccharomyces cerevisiae* CJM 567, isogenic to W303 (Livas *et al.*, 2011), *Saccharomyces cerevisiae* CEN.PK113-7D (Euroscarf), *Kluyveromyces marxianus* CBS6556 (Centraalbureau voor Schimmelcultures) and *Rhodosporidium toruloides* CCT0783 (Fundação André Tosello).

All experiments were performed in a minimal mineral medium containing 10 g of glucose, 5 g of $(NH_4)_2SO_4$, 3 g of KH_2PO_4, and 0.5 g of $MgSO_4 \cdot 7H_2O$ per litre, in addition to 1 ml of trace elements solution and 1 ml of vitamin solution. The trace element solution contained, per litre (pH = 4), EDTA (sodium salt), 15.0 g; $ZnSO_4 \cdot 7H_2O$, 4.5 g; $MnCl_2 \cdot 2H_2O$, 0.84 g; $CoCl_2 \cdot 6H_2O$, 0.3 g; $CuSO_4 \cdot 5H_2O$, 0.3 g; $Na_2MoO_4 \cdot 2H_2O$, 0.4 g; $CaCl_2 \cdot 2H_2O$, 4.5 g; $FeSO_4 \cdot 7H_2O$, 3.0 g; H_3BO_3, 1.0 g; and KI, 0.10 g. The vitamin solution contained, per litre (pH = 6.5), biotin, 0.05 g; p-amino benzoic acid, 0.2 g; nicotinic acid, 1 g; Ca pantothenate, 1 g; pyridoxine-HCl, 1 g; thiamine-HCl, 1 g; and myoinositol, 25 g. (Kumar and Lahtvee, 2020) The culture medium pH was adjusted to 6 with 1.9 ml per litre of 2 M KOH. KOH was chosen because potassium ions were already being present at high enough concentration so that addition of KOH did not change the overall concentration significantly. Final K^+ concentration in the minimal medium was 25 mM. KCl and NaCl salts were used to achieve the required concentration of K^+ and Na^+. Physiology characterization experiments were conducted using 50 mL flasks with vented caps with 20 mL of culture medium. If necessary, for downstream processing, cells were washed with 0.9% saline solution .

All strains were stored at -80ºC in a mixture of 50% YPD (1% Yeast Extract, 1% peptone, 2% glucose) and 50% glycerol. For all the experiments, cells were pre-cultured in YPD overnight, washed and then grown in minimal medium with 1% glucose for 6 hours. Afterwards, cells were washed again and inoculated in a required medium to obtain initial OD of 0.1. Four concentrations were used for experiments with single cations: 0.5, 1, 1.5 and 2 M of Na^+ or K^+. For experiments with combined cations 1 M of Na^+ was used with K^+ concentrations of 0.0025, 0.0050, 0.0075, 0.1, 0.2, 0.3, 0.4, 0.5 or 0.6 M. Not all concentrations were tested for all yeasts. Cultivation temperature was maintained at 30ºC and mixing at 200 RPM. Conditions were aerobic.

3.1.2 OD measurement

Hitachi U-1800 spectrophotometer and SARSTEDT polystyrene cuvettes were used. 0.5 or 1 mL of growth medium diluted to OD in the range of 0.05 – 0.3 was used for OD measurement. Distilled water was used as a blank.

3.1.3 Measurement of external metabolites

0.25 mL of sample was collected for each data point of interest. In preparation for high-performance liquid chromatography, samples were centrifuged twice at 11000 G and each time transferred to a new tube to remove the cells. Afterwards, samples were diluted 10 times to decrease the salt concentration. 60 µL of a diluted sample was used for measurements.

In brief, the Aminex HPX-87H chromatography column (Bio-Rad) was used with the recommended settings for elution of sugars and organic acids (temperature 45°C; flow rate 0.6 ml/min using mobile phase of 5 mM sulfuric acid) in a refractive index and UV detector containing HPLC instrument (Prominence-I, LC-2030 C Plus, SHIMADZU). (Kumar and Lahtvee, 2020)

3.1.4 Microplate reader setup

Cells were pre-cultured as described above in the "Strains and culture conditions" section. Each well was filled with 200 µL of culture medium having a starting OD of 0.1 at the start of experiment.

A BioTek Synergy MX microplate reader equipped with a shaker and a temperature control unit was used and controlled by Gen5 ver. 2.04 software. Following settings for software were used: absorbance measurement at 600 nm every 30 minutes, temperature at 30^0C and high shaking speed. The absorbance data was exported to a MS Excel for processing.

3.1.5 Specific growth rate measurement

Exponential curve was fit to a region indicating an exponential growth of the culture and reproducible data were considered for calculations when an R^2 of at least 0.95 was present. Slope of the curve was taken as a specific growth rate.

3.1.6 Image analysis pipeline for a quantitative evaluation of cell volume distribution

Cells were pre-cultured as described above in the "Strains and culture conditions" section. Cells were taken for imaging during mid-exponential phase as determined by OD

measurements. 1 mL of growth medium with cells was taken and centrifuged at 3000 G to get a cell pellet. Cells were taken from the pellet in 3 µL of volume, which was spread on a glass slide. Nikon Eclipse Ci-L microscope was used at Ph3 setting. Pictures were taken using Samsung Galaxy S7 Edge.

Custom neural network-based analysis software pipeline was developed in MATLAB and used for segmenting cells in images. Cell volume (fL) was estimated by computing major and minor axis for each cell and estimating its volume using an assumption that cells were ellipsoid. Mode was used as a representative measure of cell volume to indicate prevalence of the most common volume distribution value in the data. If multiple peaks were present, then the mode of the peak with the highest volume was used. The peaks with the smallest volume were considered to be buds, while the peaks with the largest volume – mother cells. Cell volume distributions were smoothed using Savitzky-Golay filter with polynomial degree of 8 for *S. cerevisiae* W303 and *K. marxianus* and 5 for other yeasts before mode computation. Higher degree polynomial provided more accurate mode estimation for narrow peaks of *S. cerevisiae* W303 and *K. marxianus*. Since the normal distribution was absent, a standard deviation represented in error bars was calculated independently for each half of volume distributions, which were split in two halves according to respective modes.

3.1.7 Phylogeny, DNA and protein sequence analysis

phyloT was used for building a phylogenetic tree. (Letunic, 2015)

NCBI nucleotide and protein BLAST was used to calculate homology between genes and proteins. (Johnson *et al.*, 2008) Following resources were used for obtaining DNA sequences and proteins: *S. cerevisiae* CEN.PK-113-7D (Nijkamp *et al.*, 2012), *S. cerevisiae* W303 (Matheson, Parsons and Gammie, 2017), *K. marxianus* (Lertwattanasakul *et al.*, 2015), *R. toruloides* (Zhu *et al.*, 2012).

3.2 RESULTS

3.2.1 Analysis of cationic transporters in conventional and non-conventional yeasts

Monovalent cation transporters were analyzed in both conventional and non-conventional yeasts. (Table 1, 2) *S. cerevisiae* W303 and CEN.PK strains showed different copy number of P-type ATPase sodium pumps that are involved in Na^+ and Li^+ efflux (ENA transporters). W303 strain contained four ENA genes, while CEN.PK had only a single encoding gene *ENA6*. This uniqueness makes CEN.PK highly sensitive to Na^+ stress. (Daran-Lapujade *et al.*, 2009) Though most proteins have the same amino acids sequences between W303 and CEN.PK strains, a significant number of different amino acids were found for the potassium importers Trk1p and Trk2p, which had 98.87% and 99.66% identity. (Table 2) Some of the different amino acids were close to amino acids critical for function. (Zayats *et al.*, 2015) Interestingly, *K. marxianus* had only one copy of Trk family transporter, while *R. toruloides* had both Trk1p and Trk2p. Non-conventional yeasts had two unique transporters. The Hak family transporters were found in both *K. marxianus* and *R. toruloides*, while Acu family was present only in *R. toruloides*, which also showed twice the number of main plasma membrane K^+ and Na^+ exporters, namely Tok1p and Nha1p as compared to other yeasts. (Table 1)

Organellar monovalent cation transporters in both *S. cerevisiae* strains and *K. marxianus* were similar in number and families, but *R. toruloides* lacked three such transporters, namely vacuolar Vhc1p and Vnx1p, and mitochondrial Mdm38p. However, *R. toruloides* showed the presence of an additional copy of K^+ transporter Kha1p in Golgi complex (Table 1).

Table 1. Comparison of the number K^+ and Na^+ transporters present in used yeast strains.

Transporter Family	*S. cerevisiae* (W303)	*S. cerevisiae* (CEN.PK)	*K. marxianus*	*R. toruloides*
PLASMA MEMBRANE				
Influx				
Trk family (K^+)	2	2	1	2
Hak family (K^+)	-	-	1	1
Pho89 (Na^+)	1	1	1	1
Acu family (K^+/Na^+)	-	-	-	2
Efflux				
Tok family (K^+)	1	1	1	2?
Nha family (Na^+/K^+)	1	1	1	2
Ena family (Na^+/K^+)	4	1	1-?	1-?
INTRACELLULAR				
Influx				
Nhx family (Na^+/K^+)	1	1	1	1
Stv1 (H^+)	1	1	1	1
Vph1 (H^+)	1	1	1	1
Vnx1 (Na^+/K^+)	1	1	1	-
Vhc1 (K^+)	1	1	1?	-
Kha1 (K^+)	1	1	1	2
Mdm38 (K^+)	1	1	1	-
Mrs7 (K^+)	1	1	1	1

Table 2. Comparison of transporters of monovalent cations between the used strain. W303 is used as a reference. Number of differing nucleotides and amino acids is specified for CEN.PK.

	CEN.PK-113-7D		*K. marxianus*	*R. toruloides*
	DNA identity	Protein identity	Protein identity	Protein identity
Plasma membrane				
TRK1	99.27% 27 nucleotides	98.87% 14 amino acids	53.90%	41.76%
TRK2	99.48% 13 nucleotides	99.66% 3 amino acids	-	42.70%
TOK1	100%	100%	37.28%	34.65% & 23.59%
NHA1	100%	100%	50.60%	40.50% & 37.61%
ENA	90.80% with ENA2 310 nucleotides	94.96% with ENA2 49 amino acids	66.04% with ENA2	24.52% with ENA2
PHO89	100%	100%	60.46%	33.92%
Intracellular				
Nhx1	100%	100%	64.81%	50.98%
Stv1	99.5% 12 nucleotides	99.78% 2 amino acids	59.98%	39.45%
Vph1	100%	100%	62.50%	43.30%
Vnx1	100%	100%	55.44%	-
Vhc1	99.97% 1 nucleotide	99.92% 1 amino acid	57.52% (?)	-
Kha1	100%	100%	42.98%	41.19% and 39.35%
Mdm38	99.94% 1 nucleotide	99.83% 1 amino acid	68.91%	-
Mrs7	100%	100%	69.30%	43.17%

3.2.2 Morphological and physiological differences between conventional and non-conventional yeasts

Experiments were performed in two stages: first, using a 96-well plate platform for screening tolerance to various cation concentrations and second, using shake-flask for characterization of physiology, extracellular metabolites profile and cell volume distribution at the mid-exponential phase on glucose.

Biophysical properties of cells were defined in terms of mode cell volume and independent calculation of standard deviation for each half of a volume distribution in order to consider non-normal distribution of cell volume. This allowed to convey precise information on two of the most relevant biophysical properties, i.e., volume of a typical cell and heterogeneity at the population level. Mode cell volume is dependent on volume gain per cell cycle, while heterogeneity reflects variability in volume gain in a population. (Halter *et al.*, 2009)

Vacuoles have a crucial role in salt tolerance. (Li *et al.*, 2012) Therefore, vacuole differences between different conditions and yeast were characterized. *S. cerevisiae* W303 strain showed the highest deviation for cells larger than the mode at the reference condition. (Fig. 2D) The reason for this high cell volume heterogeneity can be attributed to the variable size of the vacuole, as can be seen on microscopy images. (Fig. 2D)

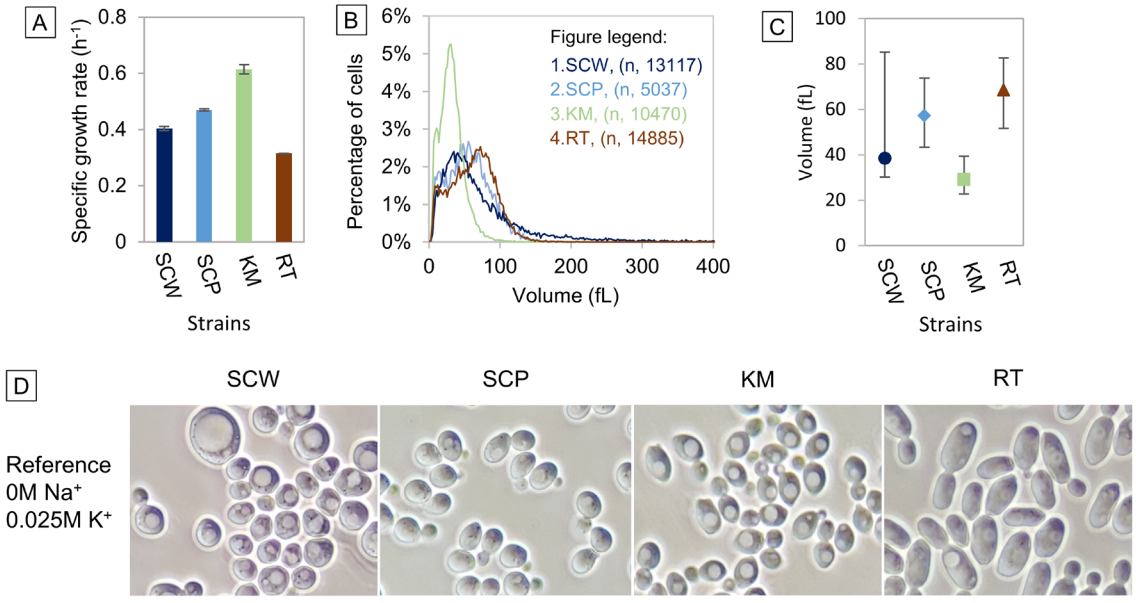

Figure 2. *S. cerevisiae* W303 (SCW, 1) (●) and CEN.PK (SCP, 2) (♦), *K. marxianus* (KM, 3) (■) and *R. toruloides* (RT, 4) (▲) in a minimal medium. Specific growth rates measured in shake-flasks. (A) Mode cell volume in the exponential growth phase and its standard deviation calculated separately for each half of a volume distribution. (B) Cell volume distributions, where N indicates the number of cells counted. (C) Microscopy pictures. (D)

3.2.3 Response to sodium ion stress

A gradient of sodium ion concentrations from 0 to 2 M was used and specific growth rates obtained using a microplate reader. (Fig. 3A) A new gradient of 0 M to 1 M was selected for comparative imaging based on obtained specific growth rates, as the growth of CEN.PK was almost negligible in concentrations of more than 1 M of sodium ions. (Fig. 3A)

Although sodium ions were increasingly toxic to all the yeasts used in the study. *S. cerevisiae* CEN.PK was especially sensitive due to the presence of only one weak *ENA* allele. (Daran-Lapujade *et al.*, 2009) (Fig. 3A)

The effect of sodium ions on cell volume distribution varied between yeasts. (Fig. 3B) Big differences in cell volume dynamics between W303 and CEN.PK were observed. Cell volume of CEN.PK increased gradually by up to 42% at 0.6 M of sodium ions and then sharply declined, reaching 114% of the initial volume at 1 M. However, W303 responded in an opposite way, its volume sharply decreased to 59% of initial volume at 0.3M of sodium ions and then slightly increased up to 80% at higher concentrations. Cell volume heterogeneity of W303 also underwent considerable changes. It initially increased peaking at 0.3M of sodium ions and then decreased abruptly at 1 M of sodium ions. Barely any cells with large vacuoles were seen at this condition. (Fig. 3C)

Non-conventional yeasts reacted differently, as *K. marxianus* showed a rapid decrease in cell volume, reaching 40% of normal at 1 M concentration, while *R. toruloides* showed the same dynamics as *S. cerevisiae* CEN.PK. (Fig. 3B) The reason for cell volume decrease of *K. marxianus* seemed to be its vacuole. *K. marxianus* had a single well pronounced vacuole at optimal conditions taking up a big part of cell volume. However, the vacuole became less pronounced and fragmented at high salinity conditions. As for *R. toruloides*, no noticeable vacuolar changes were observed. (Fig. 3C)

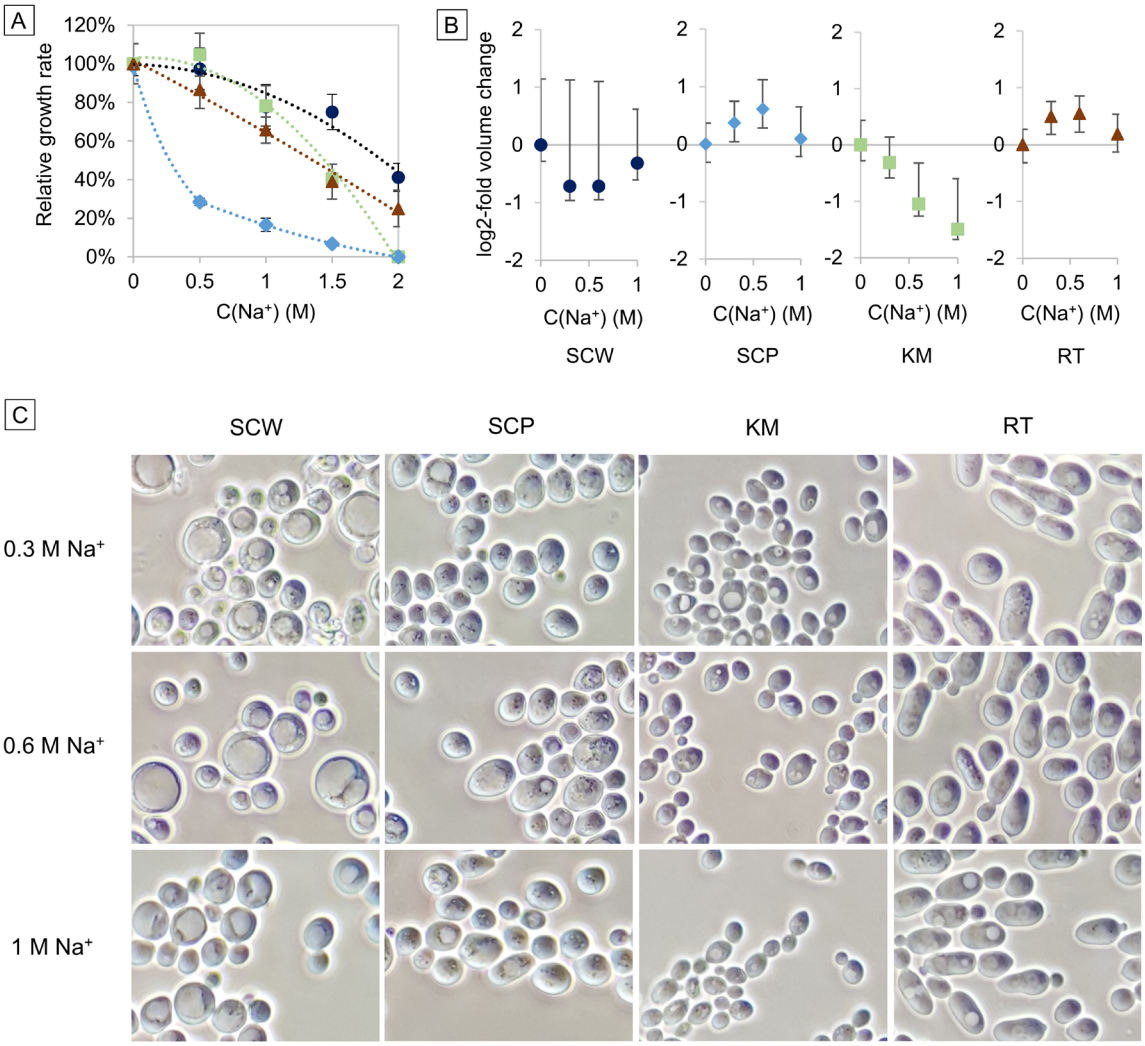

Figure 3. ***S. cerevisiae*** **W303 (SCW) (●) and CEN.PK (SCP) (♦),** ***K. marxianus*** **(KM) (■) and** ***R. toruloides*** **(RT) (▲) in a medium with different concentrations of K^+. Relative growth rates based on data from a microplate reader experiment. Growth rate at optimal conditions was taken as 100% (A). Mode relative cell volume with standard deviations in response to Na^+ caused stress. Grey line (—) – Control, Coloured markers – tested conditions. (B) Microscopy pictures. (C)**

3.2.4 Response to potassium ion stress

Similarly to sodium ion experiments, a gradient experiment using potassium ion concentrations from 0 M to 2 M was performed to obtain specific growth rates using a microplate reader. The range of the gradient for imaging was kept between 0 and 1 M based on obtained specific growth rates.

Increasing concentration of potassium ions in the growth medium appeared to be toxic to all yeasts used in the study, but less so than sodium ions in the investigated range of 0 – 1 M. Only *K. marxianus* showed more than 10% reduction in specific growth rate in the investigated range with potassium ions having a comparable toxicity to sodium ions. Interestingly, potassium ions had higher toxicity for *S. cerevisiae* W303 at 2 M concentration than sodium ions. Cells were not able to grow at all at such potassium concentration, while 40% of the normal growth rate was still observed in the presence of sodium ions. (Fig. 3A, 4A)

S. cerevisiae CEN.PK and W303 showed similar cell volume dynamics towards potassium ion stress as towards sodium ion stress. Cell volume of W303 showed a decrease followed by an increase, while this was reversed for CEN.PK. (Fig. 4B). Potassium at 1M concentration increased the number of cells with big vacuoles for W303, which can be seen from an increase in heterogeneity and microscopy pictures. (Fig. 4B, 4C) Increasing potassium concentration also caused vacuoles of W303 and CEN.PK to become misshapen.

Cell volume of *K. marxianus* reacted the same way towards potassium ions as towards sodium ions showing a drastic decrease to one third of its initial volume. Vacuoles of *K. marxianus* lost their round shape, looked rather deflated and fragmentated. *R. toruloides*, on the other hand, showed only slight increase of about 12% at 1 M of potassium ions. No vacuolar changes were observed for this strain. (Fig. 4C)

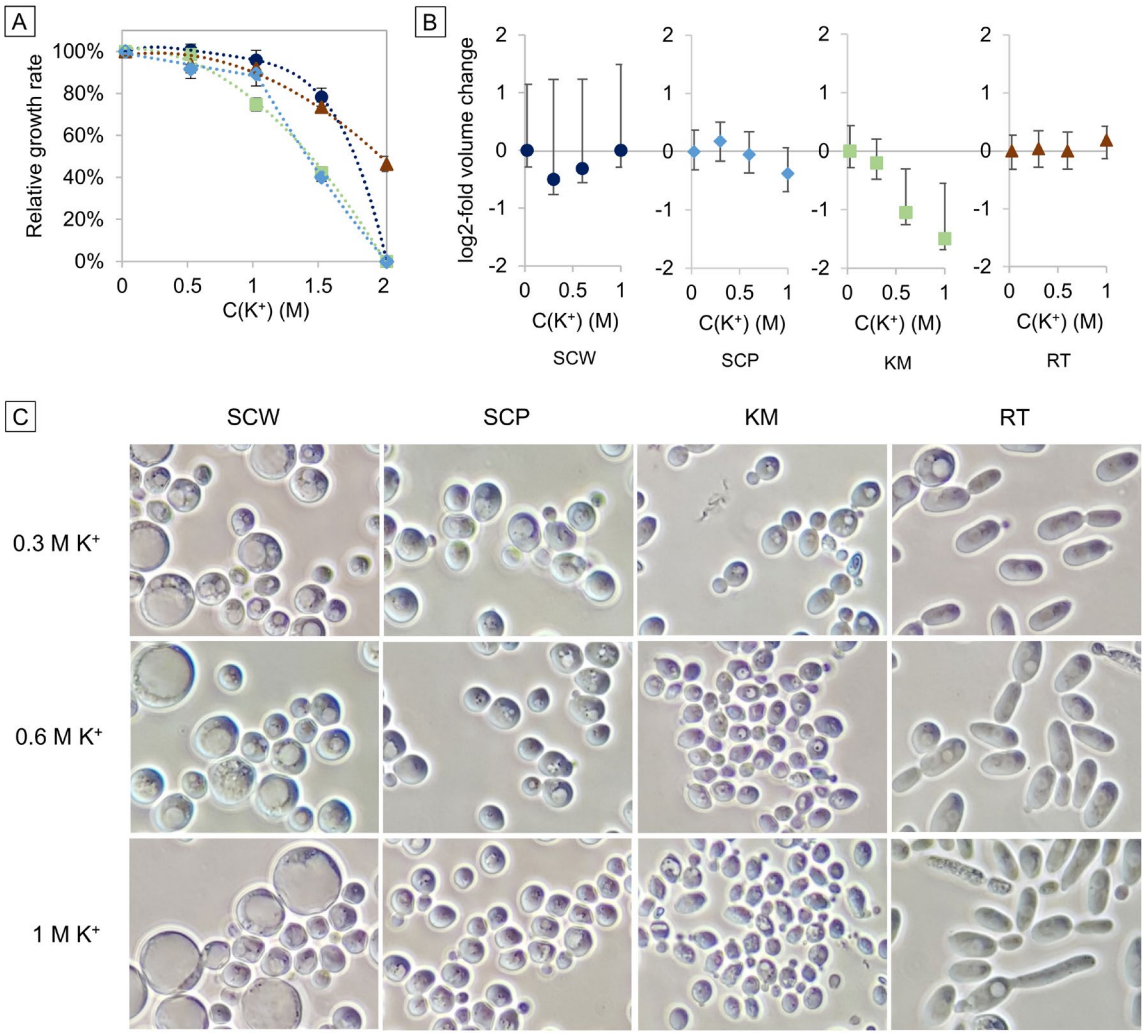

Figure 4. ***S. cerevisiae*** **W303 (SCW) (●) and CEN.PK (SCP) (♦),** ***K. marxianus*** **(KM) (■) and** ***R. toruloides*** **(RT) (▲) in a medium with different concentrations of K^+. Relative growth rates based on data from a microplate reader experiment. Growth rate at optimal conditions was taken as 100% (A). Mode cell volume with standard deviations in response to K^+ caused stress. Grey line (—) – Control, Coloured markers – tested conditions. (B) Microscopy pictures. (C)**

3.2.5 Response to a combination of sodium and potassium ion stress

The crosstalk of sodium and potassium was investigated in the background concentration of 1 M Na^+ while using a gradient of potassium ion concentrations from 0.025 M to 0.6 M.

Potassium ions increased tolerance of *S. cerevisiae* CEN.PK by almost four-fold, while having a small negative effect on *S. cerevisiae* W303 and *R. toruloides* and causing severe toxicity in *K. marxianus*. (Fig. 5A)

The final optical density (OD), which is correlated with biomass, underwent a linear decrease from 3 to 2.5 for CEN.PK with an increase in potassium ion concentration from 0.025 to 0.6 M. The decrease in OD was more drastic for other strains. (Fig. 5B)

Another metric that was affected by increased potassium ion concentration was the lag phase, which was reduced for *S. cerevisiae* CEN.PK until 0.3 M of K^+. The lag phase increased for other strains, most significantly for *K. marxianus,* where an increase from 16 to 47 hours was observed. (Fig. 5C)

S. cerevisiae strains showed inverse cell volume dynamics during the crosstalk experiments as well. CEN.PK followed a previously observed pattern for single cation stress of an increase followed by a decrease, while the W303 showed a reverse pattern. (Fig. 5D)

Vacuolar morphology did not undergo any noticeable changes due to added potassium for both *S. cerevisiae* strains and *R. toruloides*. However, significant changes were found for *K. marxianus*. Addition of 0.2 M K^+ decreased vacuolar fragmentation and increased vacuolar volume. However, further increase in concentration of K^+ caused vacuoles to shrink and become non-noticeable. (Fig. 5D)

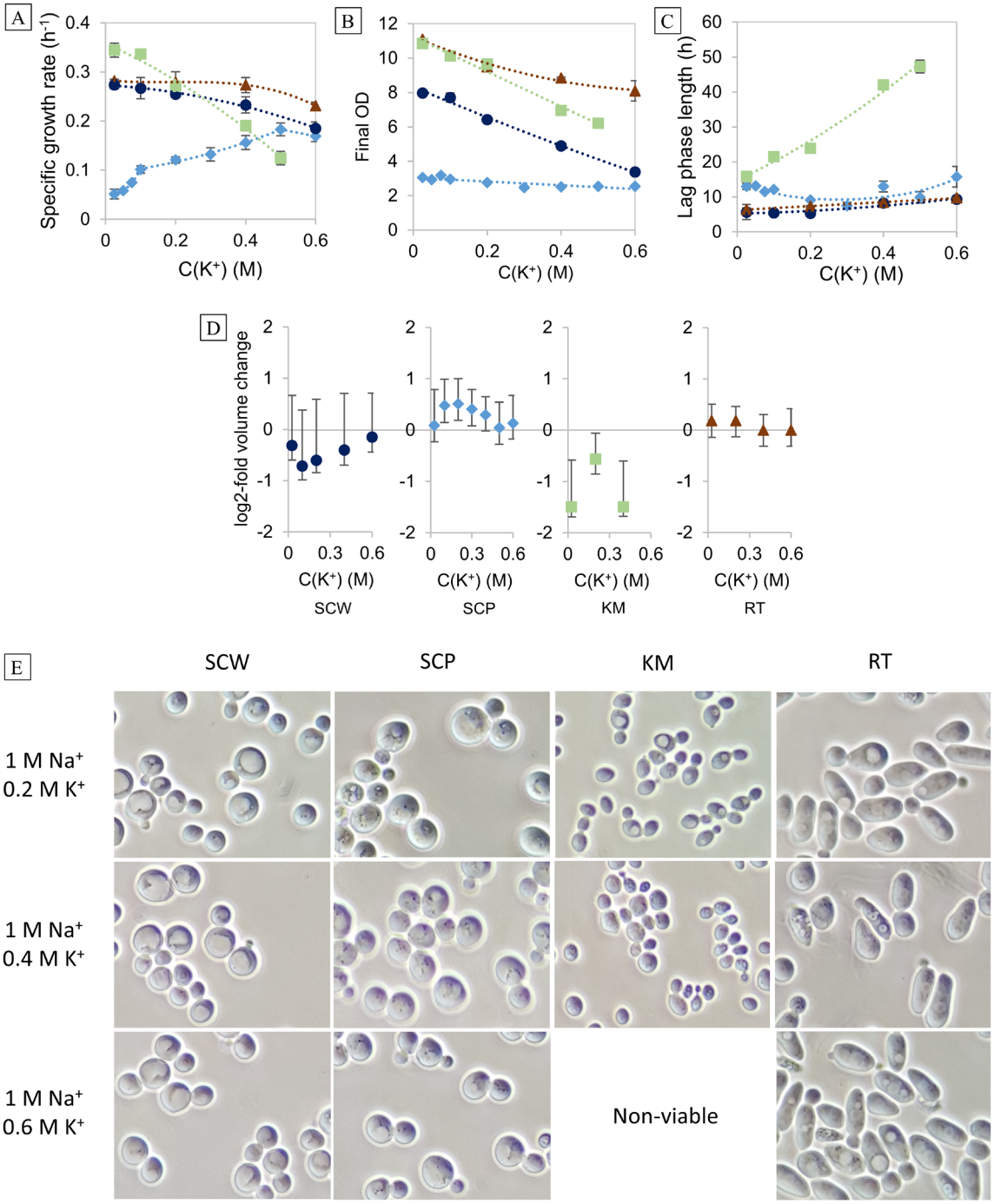

Figure 5. ***S. cerevisiae*** **W303 (SCW) (●) and CEN.PK (SCP) (♦),** ***K. marxianus*** **(KM) (■) and** ***R. toruloides*** **(RT) (▲) in a medium with 1 M of Na^+ and different concentrations of K^+: specific growth rates (A), final O.D (A), the length of a lag phase (A) based on data from shake-flaks experiments and microscopy pictures Error bars represent standard deviation.**

3.2.6 Distinct physiological response of *S. cerevisiae* W303 and CEN.PK to salt stress

Though different responses to salt stress among different species were expected, it was intriguing to notice varying responses between *S. cerevisiae* strains. External metabolite fluxes were quantified to further understand the physiology of the W303 and CEN.PK. Experimental conditions reflected those used in the study of crosstalk of salt stress, because CEN.PK showed an unusual growth rate pattern at those conditions, where growth rate increased with increasing potassium concentration. Data was collected for conditions with 1 M Na^+ and either 0.025, 0.1 or 0.5 M of K^+.

CEN.PK and W303 showed similar extracellular metabolic profiles at the reference condition without any additional salt. The only noticeable difference was 2.5 times higher acetic acid production by CEN.PK. (Fig. 6)

Slower glucose utilisation and lower maximum ethanol concentration was observed for CEN.PK compared to W303, which was consistent with its slower growth. Maximum glycerol concentration was much higher than reference for all salt stress conditions, which was an expected behaviour due to its role in osmoregulation. CEN.PK consistently accumulated more glycerol than W303. (Fig. 6)

Interestingly, two unusual patterns were noticeable in extracellular metabolite data. Firstly, CEN.PK was not able to consume acetic acid in any of the tested conditions. Due to that fact, about seven times higher acetic acid accumulation compared to the reference condition was observed, indicating that acetic acid metabolism was negatively impacted by salt stress. W303 also showed the same behaviour, but only at 0.5M of K^+, where it was unable to consume acetic acid. At the same concentration of 0.5M of K^+ CEN.PK not only did not consume acetic acid but was also unable to consume ethanol. (Fig. 6)

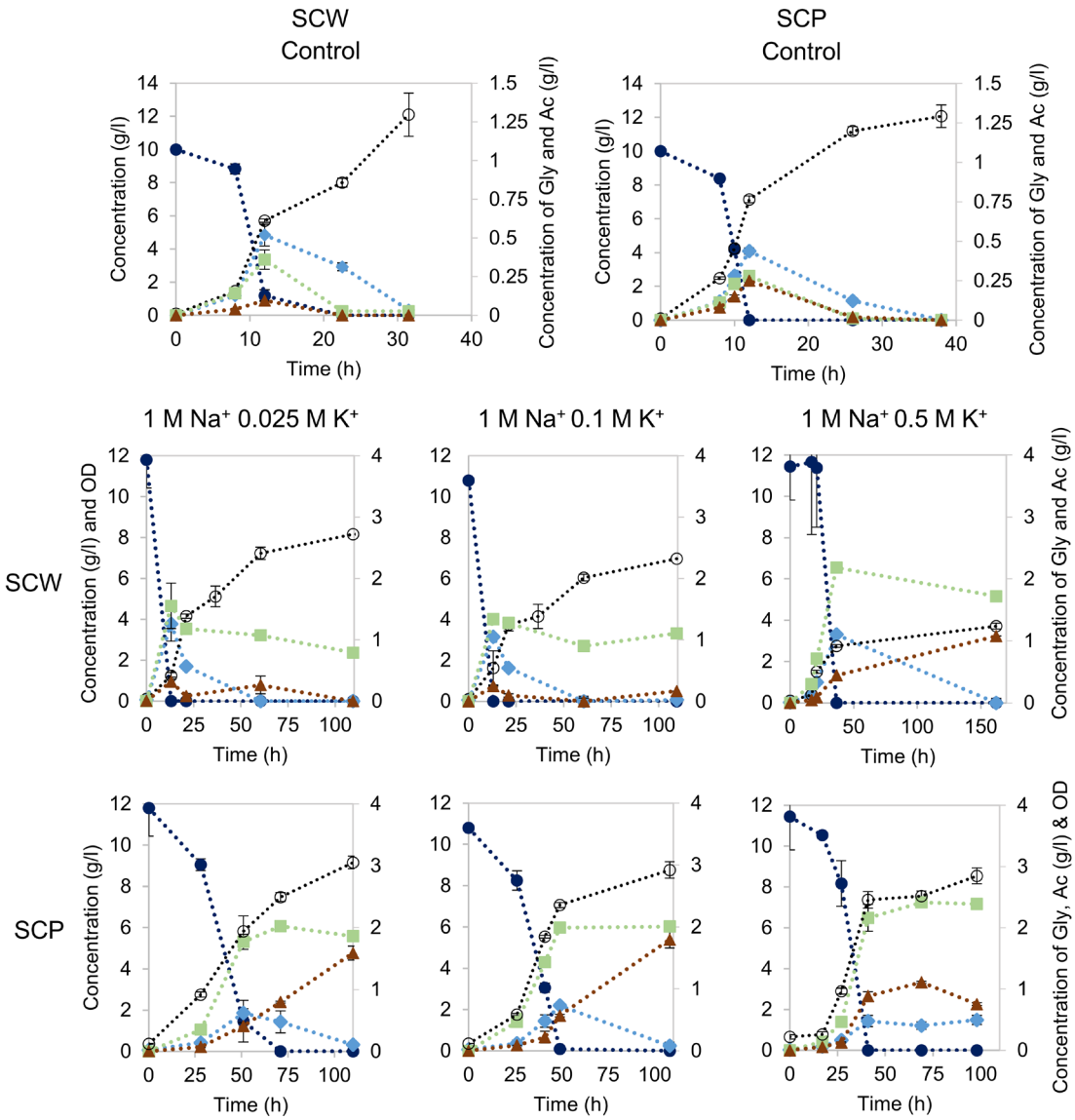

Figure 6. Growth and metabolite profiling for *S. cerevisiae* W303 (SCW) and CEN.PK (SCP) in minimal medium. Black empty circle (○) – OD, dark blue circle (●) – Glucose, light blue rhomb (♦) – ethanol, green square (■) – glycerol, brown triangle (▲) – acetic acid. Glycerol and acetic acid are on a secondary axis.

3.3 DISCUSSION

The present thesis focused on characterization of physiological and morphological parameters impacted by salt stress in four different yeasts, in particular, cell volume and growth rate. An image analysis pipeline was developed and implemented in the thesis in order to quantify cell volume. This allowed identification of high variability in cell volume dynamics among yeasts as well as among different stress conditions. Further, salt stress response of *S. cerevisiae* strains was assessed by measuring extracellular fluxes allowing for identification of salt stress impact on acetic acid and ethanol metabolism.

S. cerevisiae W303 stood out for having a very high deviation for cells larger than mode in all tested conditions, the reason for which was largely attributable to its vacuole. (Fig. 1-4C, 5D) The vacuole ended up comprising most of the cell volume for the cells larger than the respective mode. It is known than cell volume is proportional to age and that vacuole-linked autophagy becomes increasingly dysfunctional with age, which precludes efficient break down of intravacuolar material. (Hughes and Gottschling, 2012) However, the vacuolar volume increase similar to W303 was not observed in the CEN.PK or in non-conventional yeasts. It could be that the vacuole-linked autophagy dysfunction observed in S288C and W303 is specific only for those strains and not representative of yeasts in general.

One explanation for the increase in the number of cells larger than the mode, which was observed for W303 after addition of salts, is that *S. cerevisiae* W303 preferred to sequester cations in its vacuole, but only up to a certain external concertation in case of sodium ions. (Serrano, 1996)

K. marxianus stood out the most regarding cell volume regulation during salt stress. It consistently showed an almost linear decrease with increasing salt concentration. It could be that HOG pathway, while being present, works differently in *K .marxianus*. Specifically, glycerol may not be produced in response to osmotic stress. *S. cerevisiae*, while also undergoing cell volume decrease proportional to change in growth medium osmolarity, recovers its volume thanks to glycerol accumulation. (Petelenz-Kurdziel *et al.*, 2011)

CEN.PK showed a much higher sensitivity to sodium ions than other investigated yeasts. The reason for the sensitivity is inability to efficiently pump out sodium ions. (Daran-Lapujade *et al.*, 2009) Increased specific growth rate of *S. cerevisiae* CEN.PK during sodium ions stress in response to added potassium ions could be explained by increased intracellular concentration of potassium ions leading to decreased leakage of sodium ions across the plasma membrane. (Gaxiola *et al.*, 1992) Potassium ions are much less toxic for

S. cerevisiae CEN.PK (Fig. 3A, 4A). Efficiency differences due to differences in amino acids in Trk1p and Trk2p as compared to the W303 proteins could play a role in the CEN.PK by allowing intracellular concentration of potassium ions to increase in response to increasing extracellular potassium ions.

Cytosolic enzyme Adh2p together with mitochondrial Ald4p catalyse conversion of ethanol to acetic acid, while mitochondrial Ach1 and cytosolic/nuclear Acs1p enzymes are responsible for acetic acid utilisation.(Chen *et al.*, 2012; Heit *et al.*, 2018) (Fig. 7) Inability to consume ethanol of *S. cerevisiae* strains at certain combinations of Na^+ and K^+ can be explained by disruption of oxidative phosphorylation in mitochondria. Conversion of ethanol to acetic acid is impossible without regeneration of NAD^+. The impact on acetic acid metabolism in *S. cerevisiae* strains appears to be similar to *ACH1* deletion phenotype reported before, which again implicates mitochondria. (Fleck and Brock, 2009)

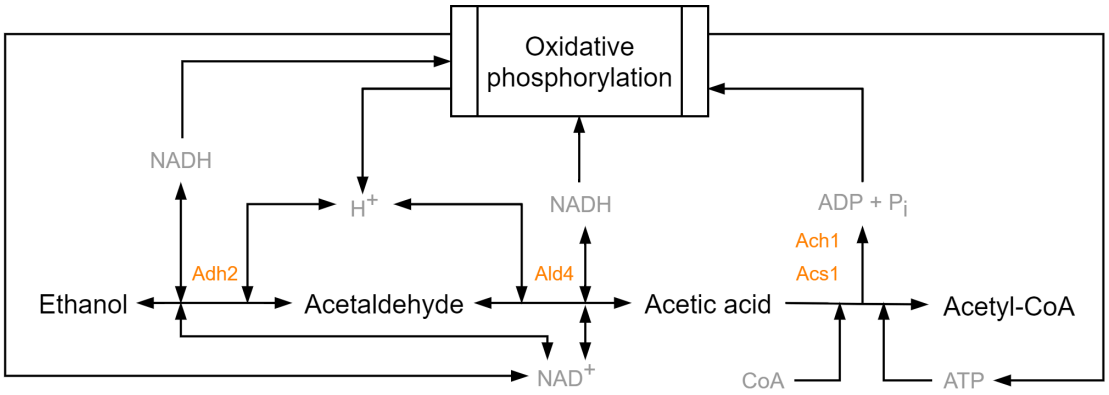

Figure 7. Pathway for ethanol utilisation.

SUMMARY

Previous studies on salt stress resistance were carried out at single cell level and in short timeframes using *S. cerevisiae* W303, S288C or their derivatives. In this thesis, *S. cerevisiae* CEN.PK strain and non-conventional yeast species in addition to W303 were used to show responses to adaptive salt stress at a population level. (Fig. 8)

There were interspecies as well as intraspecies differences in cell volume dynamics in responses to applied stressors, where vacuole played an important function. In general, cell volume regulation was not robust for all tested yeasts. Their mode cell volume, as well as heterogeneity in cell volume, was salt concentration dependent.

Results in the thesis showed differences in production and utilization of ethanol and acetic acid between W303 and CEN.PK. CEN.PK at a condition with 1 M of sodium ions as well as W303 at conditions with 1 M of sodium and 0.6 M of potassium ions were unable to consume acetic acid. Inability to consume acetic acid resulted in its accumulation during growth on ethanol. Furthermore, CEN.PK was unable to convert ethanol to acetic acid if 0.6 M of potassium ions was added in addition to 1 M of sodium ions. However, despite that, sodium ion sensitivity of *S. cerevisiae* CEN.PK was partially rescued by addition of potassium ions.

K. marxianus showed a unique behaviour regarding cell volume. Its mode cell volume decreased consistently with increased salt concentration reaching almost one third of the normal volume at 1 M sodium and potassium ion concentrations. Most of the lost volume was due to a shrunken vacuole, indicating its importance for volume regulation in the case of *K. marxianus*. Addition of potassium ions to concentration of 0.2 M allowed cell volume to partially recover. However, 0.4 M concentration did not have that effect indicating that a fine balance between sodium and potassium ions is required for *K. marxianus* to maintain its volume.

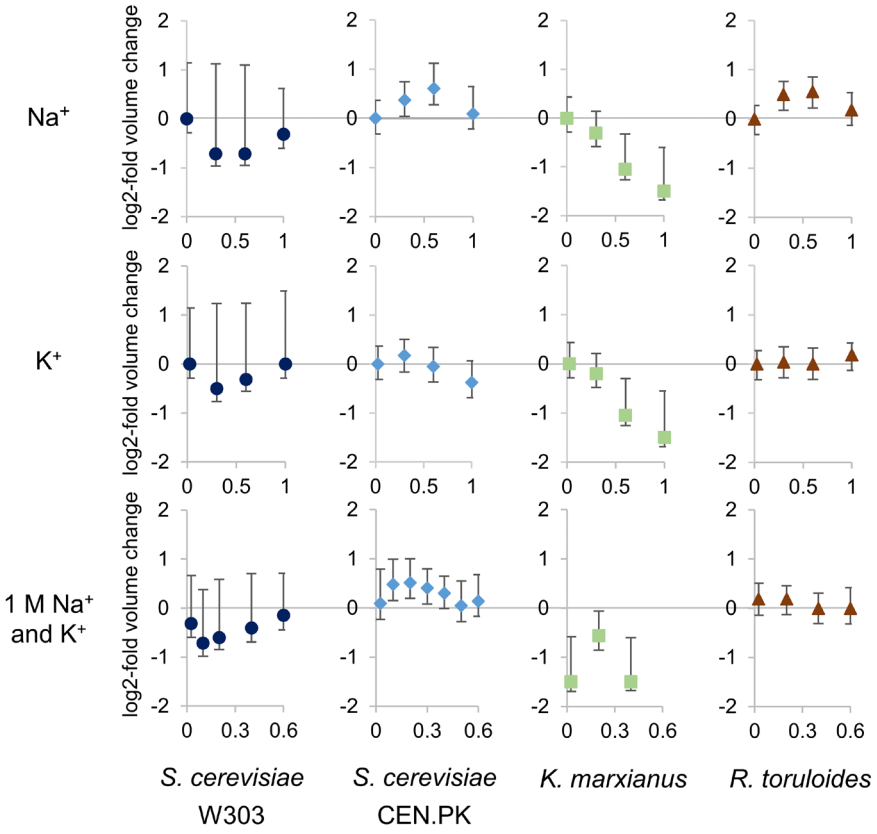

Figure 8. Cell volume change trends of *S. cerevisiae* W303 (SCW) (●) and CEN.PK (SCP) (♦), *K. marxianus* (KM) (■) and *R. toruloides* (RT) (▲) in growth media with different concentration of Na^+ and K^+ and 1 M Na^+ with different concentrations of K^+. Mode cell volumes with standard deviations are shown. Grey line (—) – control, Coloured markers – tested conditions.

ACKNOWLEDGEMENT AND FUNDING

I would like to thank Rahul Kumar and Petri-Jaan Lahtvee for supervision and members of SynBioTEC lab for their comments.

This project has received funding from the European Union's Horizon 2020 research and innovation program under grant agreement No 668997, and the Estonian Research Council (grant PUT1488P).

REFERENCES

Ahmadpour, D. *et al.* (2014) 'Yeast reveals unexpected roles and regulatory features of aquaporins and aquaglyceroporins', *Biochimica et Biophysica Acta - General Subjects*, 1840(5), pp. 1482–1491. doi: 10.1016/j.bbagen.2013.09.027.

Albert, A. *et al.* (2000) 'X-ray structure of yeast Hal2p, a major target of lithium and sodium toxicity, and identification of framework interactions determining cation sensitivity', *Journal of Molecular Biology*, 295(4), pp. 927–938. doi: 10.1006/jmbi.1999.3408.

Arino, J., Ramos, J. and Sychrova, H. (2010) 'Alkali Metal Cation Transport and Homeostasis in Yeasts', *Microbiology and Molecular Biology Reviews*, 74(1), pp. 95–120. doi: 10.1128/MMBR.00042-09.

Azambuja, S. P. H. *et al.* (2018) 'Physiology and lipid accumulation capacity of different *Yarrowia lipolytica* and *Rhodosporidium toruloides* strains on glycerol', *bioRxiv*. Cold Spring Harbor Laboratory. doi: 10.1101/278523.

Babazadeh, R. *et al.* (2013) 'Osmostress-induced cell volume loss delays yeast Hog1 signaling by limiting diffusion processes and by Hog1-specific effects', *PLoS ONE*, 8(11), pp. 1–12. doi: 10.1371/journal.pone.0080901.

Babazadeh, R. *et al.* (2017) 'The yeast osmostress response is carbon source dependent', *Scientific Reports*, 7(1), pp. 1–11. doi: 10.1038/s41598-017-01141-4.

Bellí, G. *et al.* (2001) 'Osmotic stress causes a G1 cell cycle delay and downregulation of Cln3/Cdc28 activity in *Saccharomyces cerevisiae*', *Molecular Microbiology*, 39(4), pp. 1022–1035. doi: 10.1046/j.1365-2958.2001.02297.x.

Bommareddy, R. R., Sabra, W. and Zeng, A. P. (2017) 'Glucose-mediated regulation of glycerol uptake in Rhodosporidium toruloides: Insights through transcriptomic analysis on dual substrate fermentation', *Engineering in Life Sciences*, 17(3), pp. 282–291. doi: 10.1002/elsc.201600010.

Bruinenberg, P. M. *et al.* (1986) 'A comparative radiorespirometric study of glucose metabolism in yeasts', *Yeast*. Wiley Online Library, 2(2), pp. 117–121. doi: 10.1002/yea.320020207.

Camacho, M., Ramos, J. and Rodríguez-Navarro, A. (1981) 'Potassium requirements of *Saccharomyces cerevisiae*', *Current Microbiology*, 6(5), pp. 295–299. doi: 10.1007/BF01566880.

Chen, Y., Siewers, V. and Nielsen, J. (2012) 'Profiling of cytosolic and peroxisomal acetyl-CoA metabolism in Saccharomyces cerevisiae', *PLoS ONE*, 7(8). doi: 10.1371/journal.pone.0042475.

Daran-Lapujade, P. *et al.* (2009) 'An atypical PMR2 locus is responsible for hypersensitivity to sodium and lithium cations in the laboratory strain *Saccharomyces cerevisiae* CEN.PK113-7D', *FEMS Yeast Research*, 9(5), pp. 789–792. doi: 10.1111/j.1567-1364.2009.00530.x.

Fleck, C. B. and Brock, M. (2009) 'Re-characterisation of *Saccharomyces cerevisiae* Ach1p: Fungal CoA-transferases are involved in acetic acid detoxification', *Fungal Genetics and Biology*. Elsevier Inc., 46(6–7), pp. 473–485. doi: 10.1016/j.fgb.2009.03.004.

Fonseca, G. G. *et al.* (2008) 'The yeast *Kluyveromyces marxianus* and its biotechnological potential', *Applied Microbiology and Biotechnology*, 79(3), pp. 339–354. doi: 10.1007/s00253-008-1458-6.

Gaxiola, R. *et al.* (1992) 'A novel and conserved salt-induced protein is an important determinant of salt tolerance in yeast.', *The EMBO Journal*, 11(9), pp. 3157–3164. doi: 10.1002/j.1460-2075.1992.tb05392.x.

Goddard, M. R. and Greig, D. (2015) '*Saccharomyces cerevisiae*: A nomadic yeast with no niche?', *FEMS Yeast Research*, 15(3), pp. 1–6. doi: 10.1093/femsyr/fov009.

Halter, M. *et al.* (2009) 'Cell volume distributions reveal cell growth rates and division times', *Journal of Theoretical Biology*, 257(1), pp. 124–130. doi: 10.1016/j.jtbi.2008.10.031.

Heit, C. *et al.* (2018) 'Osmoadaptation of wine yeast (*Saccharomyces cerevisiae*) during Icewine fermentation leads to high levels of acetic acid', *Journal of Applied Microbiology*, 124(6), pp. 1506–1520. doi: 10.1111/jam.13733.

Herrera, R. *et al.* (2014) 'Role of *Saccharomyces cerevisiae* Trk1 in stabilization of intracellular potassium content upon changes in external potassium levels', *Biochimica et Biophysica Acta - Biomembranes*. Elsevier B.V., 1838(1 PARTB), pp. 127–133. doi: 10.1016/j.bbamem.2013.08.022.

Hohmann, S. (2002a) 'Osmotic adaptation in yeast-control of the yeast osmolyte system', *International Review of Cytology*, 215, pp. 149–187. doi: 10.1016/S0074-7696(02)15008-X.

Hohmann, S. (2002b) 'Osmotic stress signaling and osmoadaptation in yeasts.', *Microbiology and molecular biology reviews : MMBR*, 66(2), pp. 300–372. doi: 10.1128/mmbr.66.2.300-372.2002.

Hughes, A. L. and Gottschling, D. E. (2012) 'An early age increase in vacuolar pH limits mitochondrial function and lifespan in yeast', *Nature*. Nature Publishing Group, 492(7428), pp. 261–265. doi: 10.1038/nature11654.

Jeong, H. *et al.* (2012) 'Genome sequence of the thermotolerant yeast *Kluyveromyces marxianus var. marxianus* KCTC 17555', *Eukaryotic Cell*, 11(12), pp. 1584–1585. doi: 10.1128/EC.00260-12.

Johnson, M. *et al.* (2008) 'NCBI BLAST: a better web interface', *Nucleic Acids Research*. doi: 10.1093/nar/gkn201.

Klipp, E. *et al.* (2005) 'Integrative model of the response of yeast to osmotic shock.', *Nature biotechnology*. United States, 23(8), pp. 975–982. doi: 10.1038/nbt1114.

Kumar, R. and Lahtvee, P. (2020) 'Proteome overabundance enables respiration but limitation onsets carbon overflow'. doi: 10.1101/2020.02.20.957662.

Lahtvee, P.-J. *et al.* (2016) 'Adaptation to different types of stress converge on mitochondrial metabolism.', *Molecular biology of the cell*, 27(15), pp. 2505–2514. doi: 10.1091/mbc.E16-03-0187.

Lam, F. H. *et al.* (2014) 'Engineering alcohol tolerance in yeast', *Science*, 346(6205), pp. 71–75. doi: 10.1126/science.1257859.

Lertwattanasakul, N. *et al.* (2015) 'Genetic basis of the highly efficient yeast *Kluyveromyces marxianus*: Complete genome sequence and transcriptome analyses', *Biotechnology for Biofuels*, 8(1), pp. 1–14. doi: 10.1186/s13068-015-0227-x.

Letunic, I. (2015) 'phyloT: Phylogenetic Tree Generator.', [online] phylot.biobyte.de.

Li, S. C. *et al.* (2012) 'Vacuolar H^+-atpase works in parallel with the HOG pathway to adapt *Saccharomyces cerevisiae* cells to osmotic stress', *Eukaryotic Cell*, 11(3), pp. 282–291. doi: 10.1128/EC.05198-11.

Livas, D. *et al.* (2011) 'Transcriptional responses to glucose in *Saccharomyces cerevisiae* strains lacking a functional protein kinase A', *BMC Genomics*, 12(1), p. 405. doi: 10.1186/1471-2164-12-405.

Lopez, F. *et al.* (1999) 'The yeast inositol monophosphatase is a lithium- and sodium-

sensitive enzyme encoded by a non-essential gene pair', *Molecular Microbiology*, 31(4), pp. 1255–1264. doi: 10.1046/j.1365-2958.1999.01267.x.

Matheson, K., Parsons, L. and Gammie, A. (2017) 'Whole-genome sequence and variant analysis of W303, a widely-used strain of *Saccharomyces cerevisiae*', *G3: Genes, Genomes, Genetics*, 7(7), pp. 2219–2226. doi: 10.1534/g3.117.040022.

Mitchell, A., Wei, P. and Lim, W. A. (2015) 'Oscillatory stress stimulation uncovers an Achilles' heel of the yeast MAPK signaling network', *Science*, 350(6266), pp. 1379–1383. doi: 10.1126/science.aab0892.

Nass, R. and Rao, R. (1999) 'The yeast endosomal Na^+/H^+ exchanger, Nhx1, confers osmotolerance following acute hypertonic shock', *Microbiology*, 145(11), pp. 3221–3228. doi: 10.1099/00221287-145-11-3221.

Nielsen, J. (2015) 'BIOENGINEERING. Yeast cell factories on the horizon.', *Science (New York, N.Y.)*. United States, 349(6252), pp. 1050–1051. doi: 10.1126/science.aad2081.

Nijkamp, J. F. *et al.* (2012) 'De novo sequencing, assembly and analysis of the genome of the laboratory strain *Saccharomyces cerevisiae* CEN.PK113-7D, a model for modern industrial biotechnology', *Microbial cell factories*. Springer, 11(1), p. 36. doi: 10.1186/1475-2859-11-36.

Ostergaard, S., Olsson, L. and Nielsen, J. (2000) 'Metabolic Engineering of *Saccharomyces cerevisiae*', 64(1), pp. 34–50.

Park, Y.-K., Nicaud, J.-M. and Ledesma-Amaro, R. (2018) 'The engineering potential of *Rhodosporidium toruloides* as a workhorse for biotechnological applications', *Trends in biotechnology*. Elsevier, 36(3), pp. 304–317. doi: 10.1016/j.tibtech.2017.10.013.

Petelenz-Kurdziel, E. *et al.* (2011) 'Quantification of cell volume changes upon hyperosmotic stress in *Saccharomyces cerevisiae*', *Integrative Biology*, 3(11), pp. 1120–1126. doi: 10.1039/c1ib00027f.

Qian, J. *et al.* (2011) 'Cloning and characterization of *Kluyveromyces marxianus* Hog1 gene', *Biotechnology Letters*, 33(3), pp. 571–575. doi: 10.1007/s10529-010-0458-7.

Ralser, Markus *et al.* (2012) 'The *Saccharomyces cerevisiae* W303-K6001 cross-platform genome sequence: insights into ancestry and physiology of a laboratory mutt', *Open biology*. The Royal Society, 2(8), p. 120093. doi: 10.1098/rsob.120093.

Rodríguez-Navarro, A. (2000) 'Potassium transport in fungi and plants', *Biochimica et*

Biophysica Acta - Reviews on Biomembranes, 1469(1), pp. 1–30. doi: 10.1016/S0304-4157(99)00013-1.

Satyanarayana, T. and Kunze, G. (2017) 'Yeast Diversity in Human Welfare', *Yeast Diversity in Human Welfare*, pp. 1–486. doi: 10.1007/978-981-10-2621-8.

Schaber, J. *et al.* (2010) 'Biophysical properties of *Saccharomyces cerevisiae* and their relationship with HOG pathway activation', *European Biophysics Journal*, 39(11), pp. 1547–1556. doi: 10.1007/s00249-010-0612-0.

Serrano, R. (1996) 'Salt tolerance in plants and microorganisms: Toxicity targets and defense responses', *International Review of Cytology*, 165, pp. 1–52. doi: 10.1016/s0074-7696(08)62219-6.

Strucko, T., Magdenoska, O. and Mortensen, U. H. (2015) 'Benchmarking two commonly used *Saccharomyces cerevisiae* strains for heterologous vanillin-β-glucoside production', *Metabolic Engineering Communications*. Elsevier, 2, pp. 99–108. doi: 10.1016/j.meteno.2015.09.001.

Tiukova, I. A. *et al.* (2019) 'Genome-scale model of *Rhodotorula toruloides* metabolism', *Biotechnology and bioengineering*. Wiley Online Library, 116(12), pp. 3396–3408. doi: 10.1002/bit.27162.

Wardrop, F. R. *et al.* (2004) 'Physiological responses of Crabtree positive and Crabtree negative yeasts to glucose upshifts in a chemostat', *Annals of Microbiology*, 54(1), pp. 103–114.

Yenush, L. (2016a) 'Potassium and Sodium Transport in Yeast.', *Advances in experimental medicine and biology*. United States, 892, pp. 187–228. doi: 10.1007/978-3-319-25304-6_8.

Yenush, L. (2016b) *Yeast Membrane Transport*. doi: 10.1007/978-3-319-25304-6.

Zayats, V. *et al.* (2015) 'A refined atomic scale model of the *Saccharomyces cerevisiae* K^+-translocation protein Trk1p combined with experimental evidence confirms the role of selectivity filter glycines and other key residues', *Biochimica et Biophysica Acta - Biomembranes*. Elsevier B.V., 1848(5), pp. 1183–1195. doi: 10.1016/j.bbamem.2015.02.007.

Zhu, Z. *et al.* (2012) 'A multi-omic map of the lipid-producing yeast *Rhodosporidium toruloides*', *Nature Communications*. Nature Publishing Group, 3. doi: 10.1038/ncomms2112.

SUPPLEMENTARY

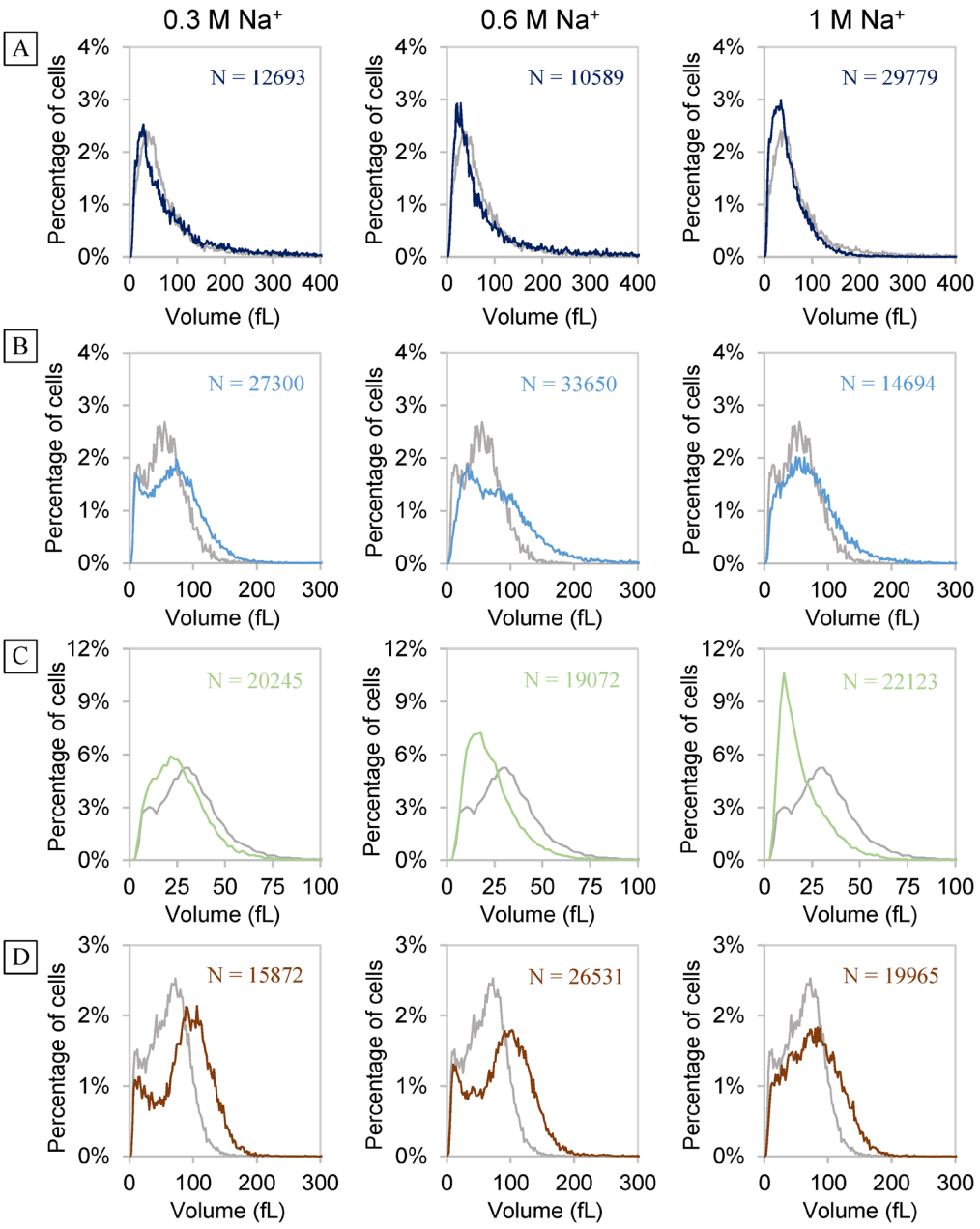

S1. Cell volume distributions of *S. cerevisiae* W303 (—) (A) and CEN.PK (—) (B), *K. marxianus* (—) (C) and *R. toruloides* (—) (D) in response to Na^+ caused stress. Grey lines (—) – Controls, Coloured lines – tested conditions.

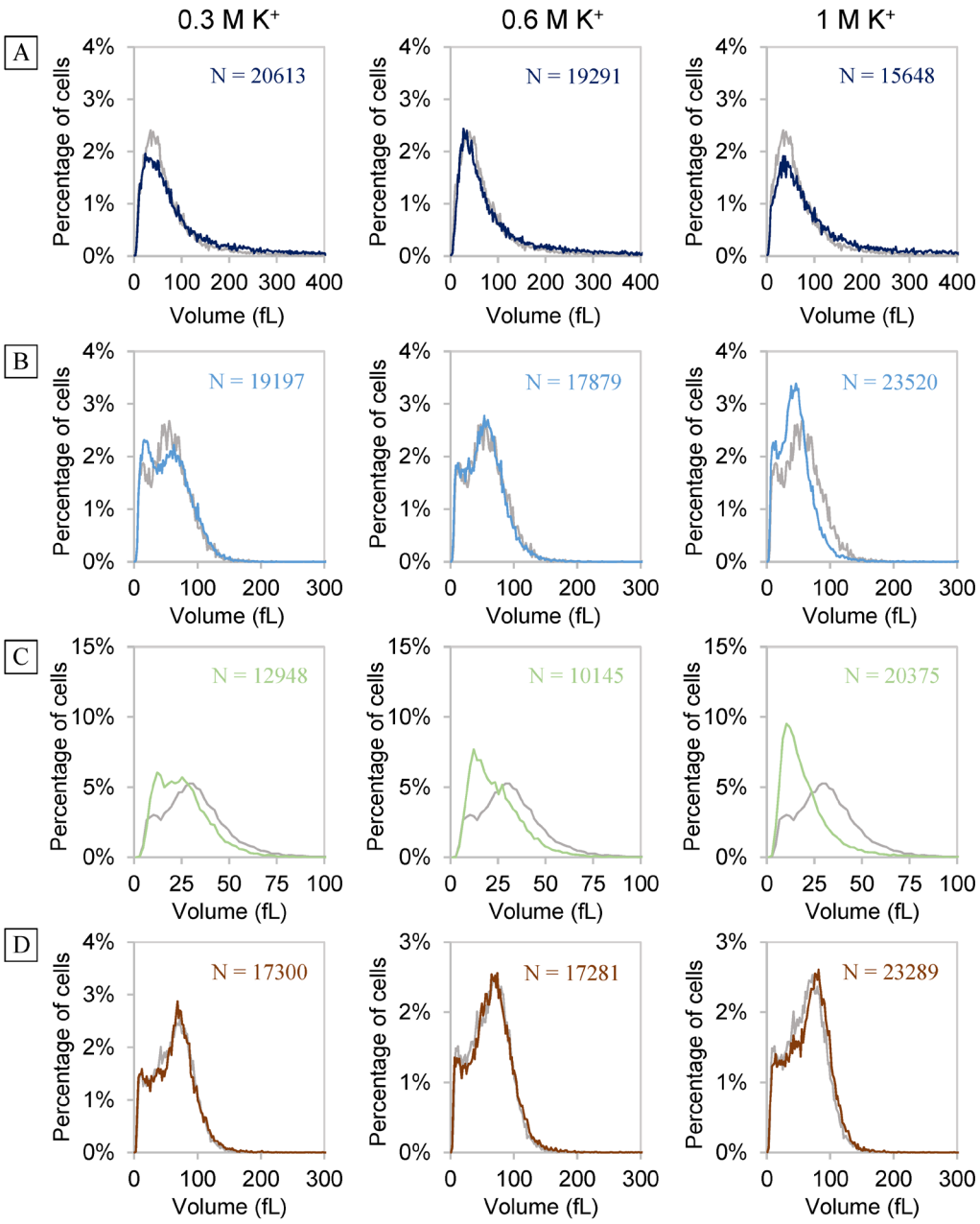

S2. Cell volume distributions of *S. cerevisiae* W303 (—) (A) and CEN.PK (—) (B), *K. marxianus* (—) (C) and *R. toruloides* (—) (D) in response to K^+ caused stress. Grey lines (—) – Controls, Coloured lines – tested conditions.

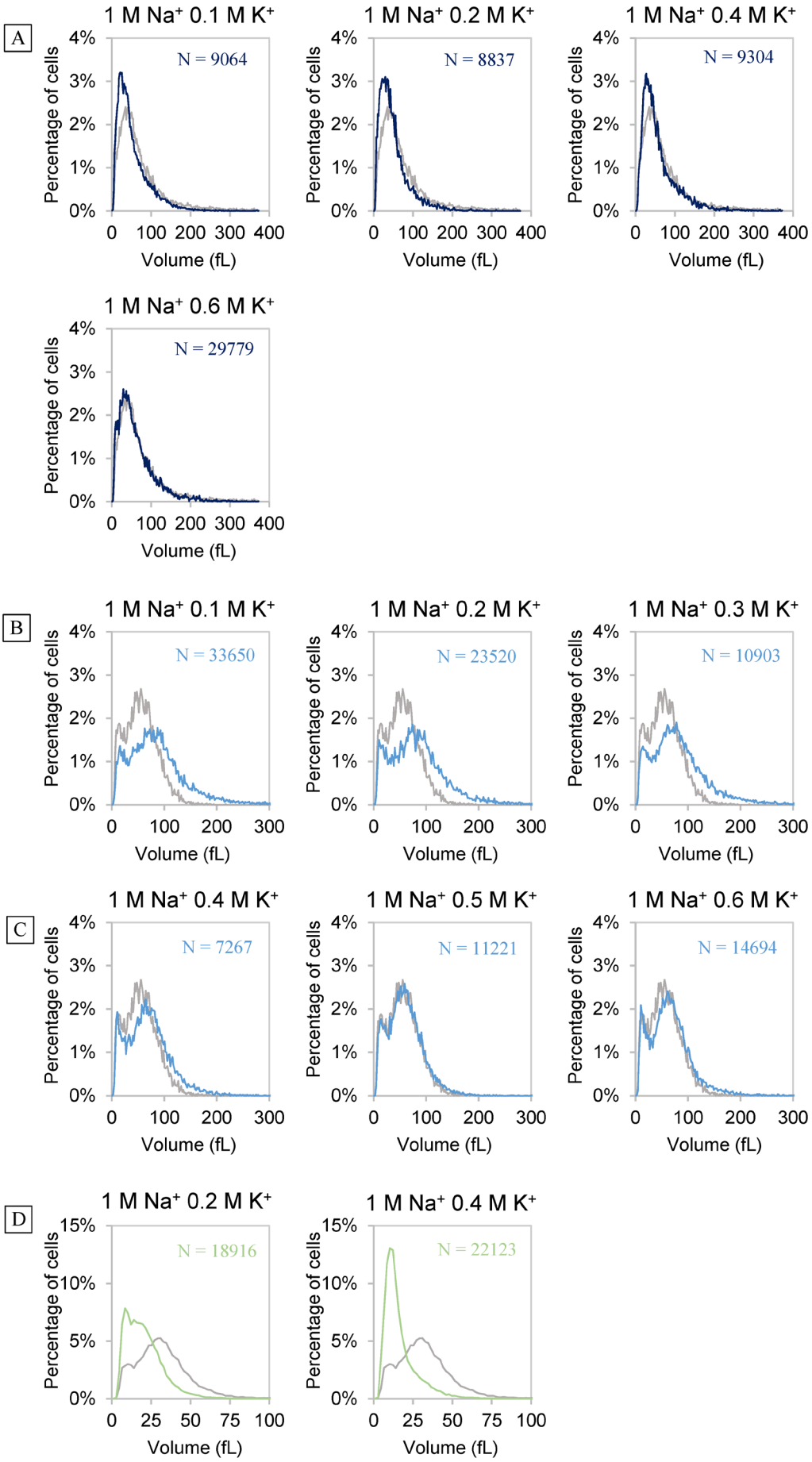
A
1 M Na+ 0.1 M K+
N = 9064
1 M Na+ 0.2 M K+
N = 8837
1 M Na+ 0.4 M K+
N = 9304
1 M Na+ 0.6 M K+
N = 29779
B
1 M Na+ 0.1 M K+
N = 33650
1 M Na+ 0.2 M K+
N = 23520
1 M Na+ 0.3 M K+
N = 10903
C
1 M Na+ 0.4 M K+
N = 7267
1 M Na+ 0.5 M K+
N = 11221
1 M Na+ 0.6 M K+
N = 14694
D
1 M Na+ 0.2 M K+
N = 18916
1 M Na+ 0.4 M K+
N = 22123
Percentage of cells
Volume (fL)

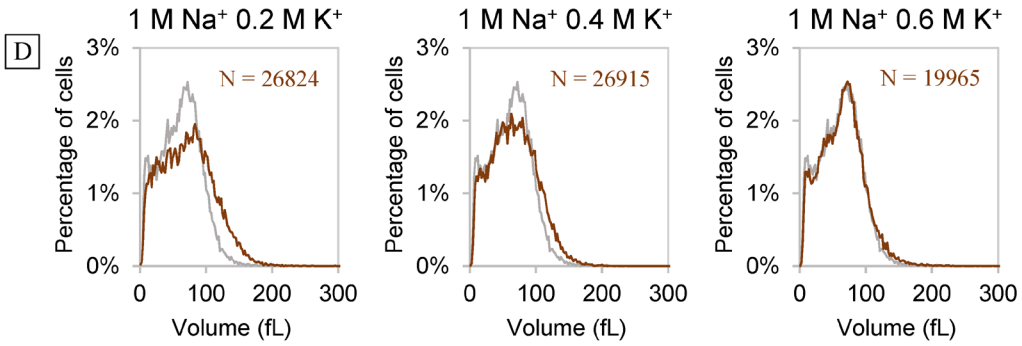

S3. Cell volume distributions of *S. cerevisiae* W303 (—) (A) and CEN.PK (—) (B), *K. marxianus* (—) (C) and *R. toruloides* (—) (D) in response to K^+ caused stress in the background of 1 M Na^+ Grey lines (—) – Controls, Coloured lines – tested conditions.

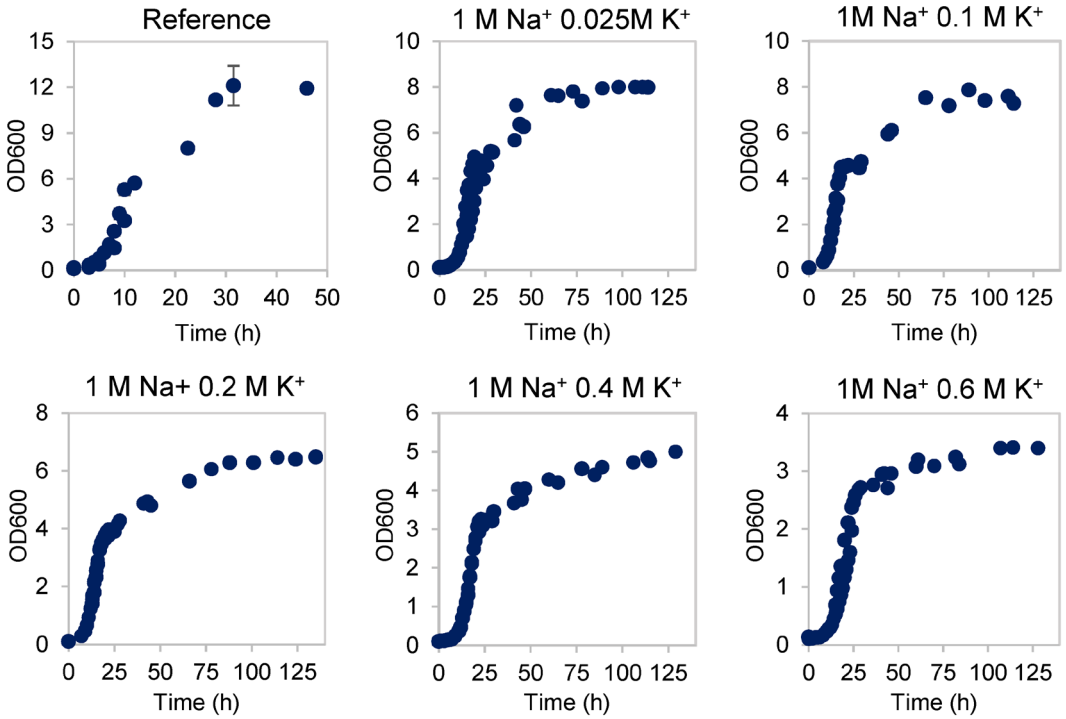

S4. Growth profiles of *S. cerevisiae* W303 (●) in minimal medium with no added salts and 1 M of Na^+ with varying concentrations of K^+.

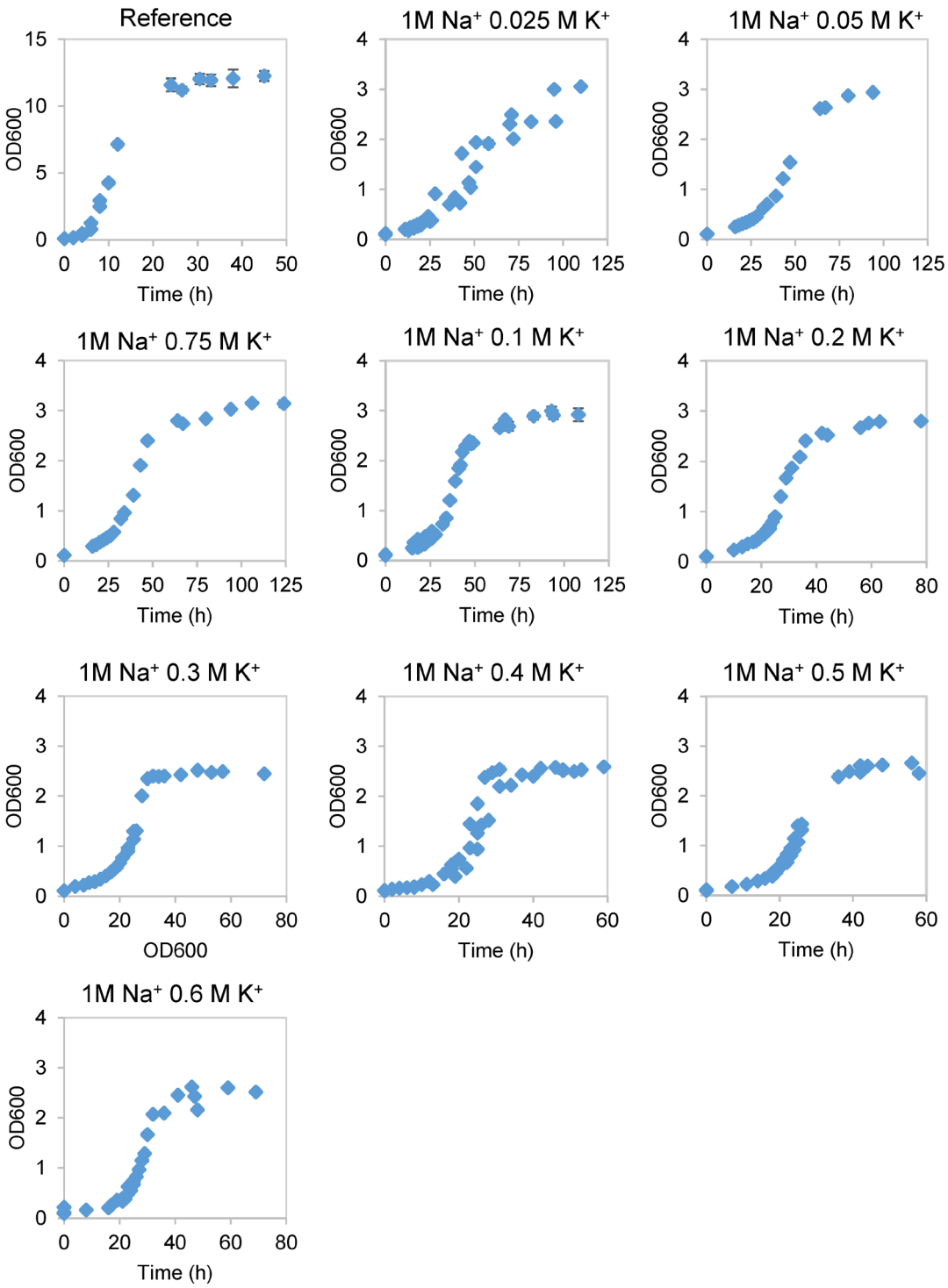

S5. Growth profiles of *S. cerevisiae* CEN.PK (♦) in minimal medium with no added salts and 1 M of Na^+ with varying concentrations of K^+.

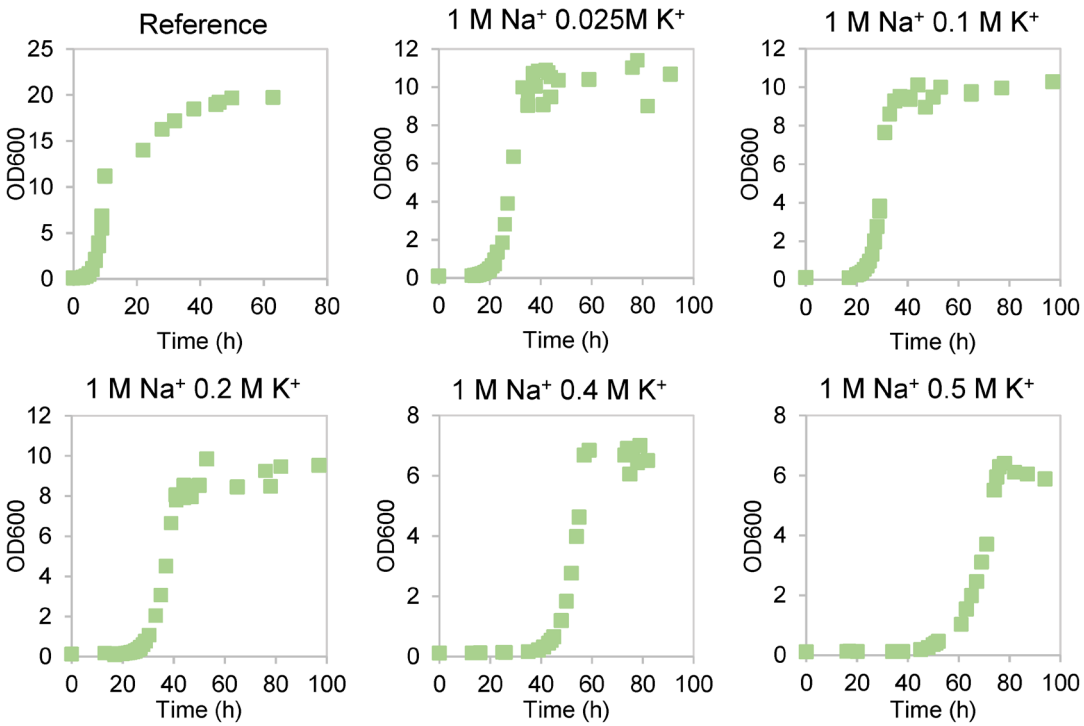

S6. Growth profiles of *K. marxianus* (■) in minimal medium with no added salts and 1 M of Na^+ with varying concentrations of K^+.

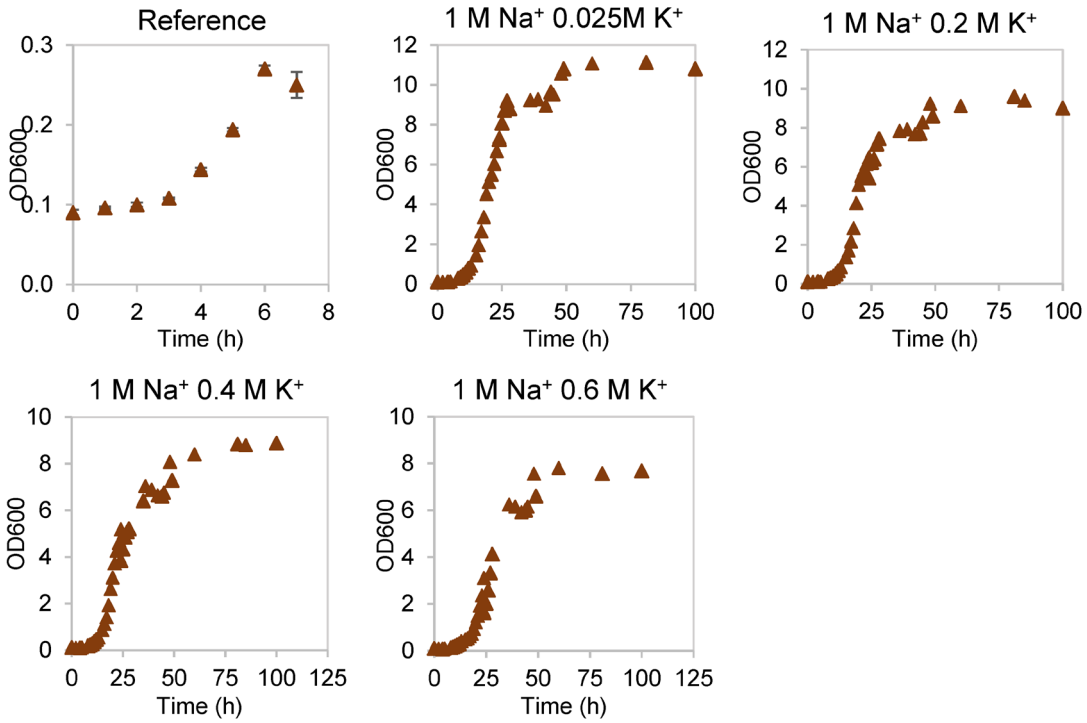

S7. Growth profiles of *R. toruloides* (▲) in minimal medium with no added salts and 1 M of Na^+ with varying concentrations of K^+.

NON-EXCLUSIVE LICENCE TO REPRODUCE THESIS AND MAKE THESIS PUBLIC

I, Aleksandr Illarionov,

1. herewith grant the University of Tartu a free permit (non-exclusive licence) to reproduce, for the purpose of preservation, including for adding to the DSpace digital archives until the expiry of the term of copyright, Quantitative evaluation of sodium and potassium salts stress in yeasts supervised by Rahul Kumar and Petri-Jaan Lahtvee.

2. I grant the University of Tartu a permit to make the work specified in p. 1 available to the public via the web environment of the University of Tartu, including via the DSpace digital archives, under the Creative Commons licence CC BY NC ND 3.0, which allows, by giving appropriate credit to the author, to reproduce, distribute the work and communicate it to the public, and prohibits the creation of derivative works and any commercial use of the work until the expiry of the term of copyright.

3. I am aware of the fact that the author retains the rights specified in p. 1 and 2.

4. I certify that granting the non-exclusive licence does not infringe other persons' intellectual property rights or rights arising from the personal data protection legislation.

Aleksandr Illarionov

20.05.2020